Computational Fluid Dynamics
Flow Data Analysis
Lecture 12

Krister Wiklund
Department of Physics
Umeå University

SUMMARY OF LECTURE: FLOW DATA ANALYSIS

- Be aware of common types of scaling in CFD-graphs
- Be aware of common test parameters that can be used to compare a CFD-model with experiments, e.g. production, diffusion, dissipation, Pk/epsilon etc.
- Be able to use y+ scaling in presentation of CFD-data
- Be aware of common definitions of Reynolds number
- Understand how the “Decaying turbulence”-case can be useful in the analysis of the Standard k-epsilon model
- Understand how the “Homogeneous shear flow”-case can be useful in the analysis of the Standard k-epsilon model
- Be aware of the “Round jet”-case

Recap: Log-layer properties in a 2D-BL

$$a)\ U^+ = \frac{1}{\kappa}\ln y^+ + 5.5$$

$$b)\ P_k = \varepsilon$$

$$c)\ -\rho\langle u'v'\rangle \approx \tau_w$$

$$d)\ \text{Exp} \Rightarrow \frac{u_\tau^2}{k} \approx 0.3$$

$$\tau_w = \rho u_\tau^2$$

$$\mu_t = C_\mu \rho \frac{k^2}{\varepsilon}$$

$$P_k \equiv \frac{R_{ij}}{\rho}\frac{\partial U_i}{\partial x_j} = 2\frac{\mu_t}{\rho}S_{ij}S_{ij}$$

Useful tools:

a) ➡ $\frac{\partial U}{\partial y} = \frac{u_\tau}{\kappa y}$ (1)

b) ➡ $\frac{\mu_t}{\rho}\left(\frac{\partial U}{\partial y}\right)^2 = \varepsilon$ (2)

c) ➡ $P_k \approx u_\tau^2 \frac{\partial U}{\partial y}$ (3)

Wall functions boundary conditions

$$k = \frac{u_\tau^2}{\sqrt{C_\mu}} \qquad \varepsilon = \frac{u_\tau^3}{\kappa y}$$

- In the viscous sublayer the production goes to zero at the boundary
- In the log-layer the production decreases for large wall distances

This means that the production has a maximum somewhere in the Buffer layer.

The Buffer layer thus contain the highest turbulence activity

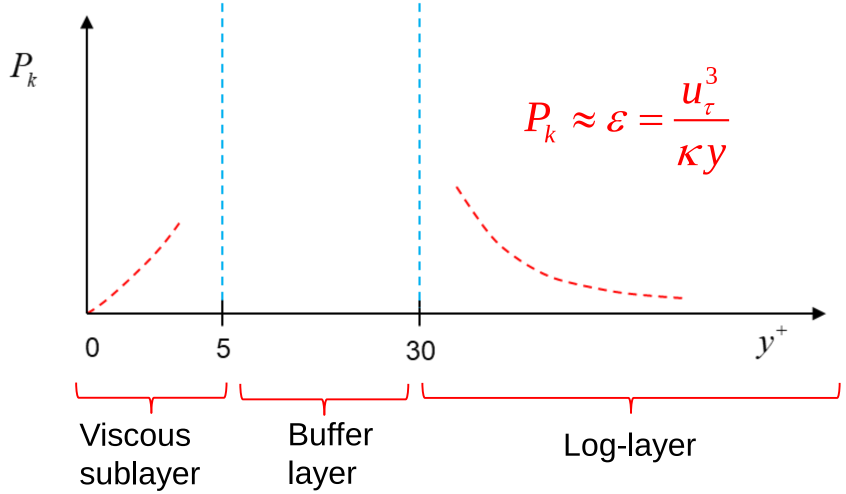

The k-eq. lab: DNS-near wall velocity profile

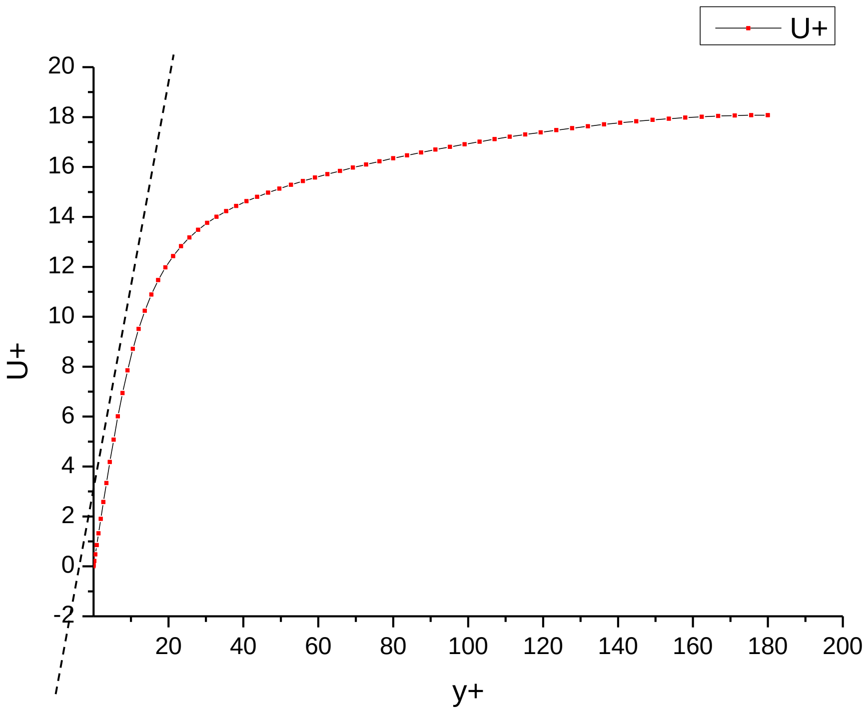

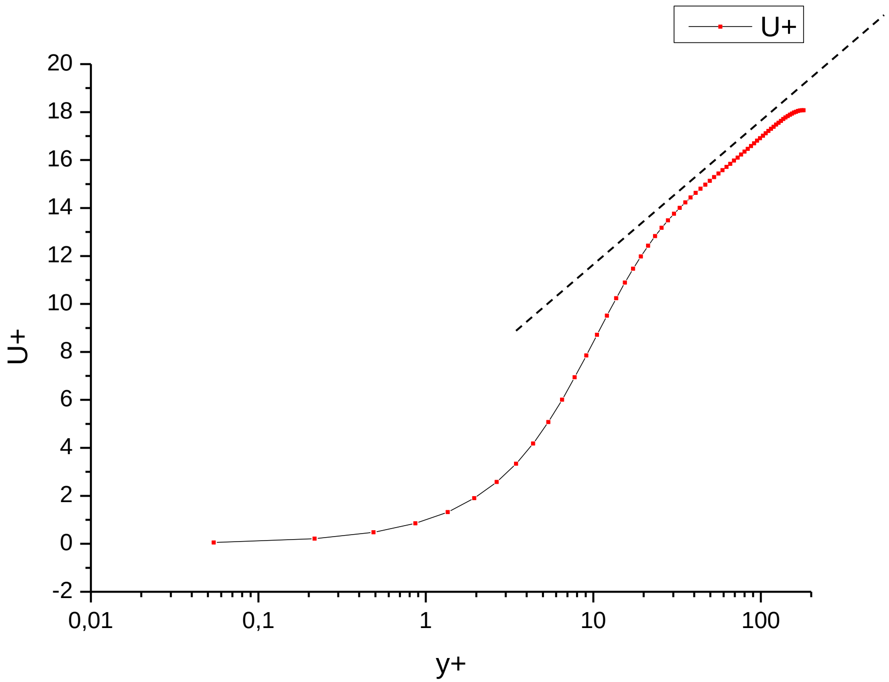

$$\boxed{U^+ \equiv \frac{U}{u_\tau}}$$

$$\boxed{y^+ \equiv \frac{\rho u_\tau y}{\mu}}$$

Friction velocity

$$u_\tau \equiv \sqrt{\tau_w / \rho}$$

τ_w = wall shear stress

Dimensionless universal scaling near wall ➡ Universally valid plots

Turbulent boundary layer velocity profiles

Viscous sublayer

$$\boxed{U^+ = y^+, \quad y^+ \le 5}$$

$$\boxed{U^+ \equiv \frac{U}{u_\tau}, \; y^+ \equiv \frac{\rho u_\tau y}{\mu}}$$

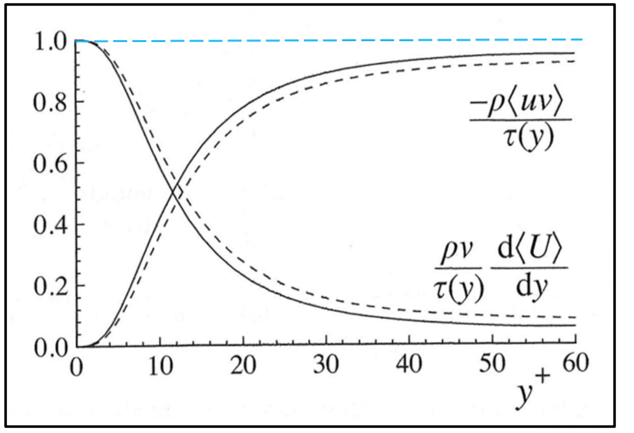

$$\boxed{y^+ \le 5: \;\; \tau \approx \tau_w}$$

$$\tau_w = \rho u_\tau^2$$

$$\mu \frac{dU}{dy} = \tau_w \Rightarrow \frac{\mu}{\rho}\frac{dU}{dy} = u_\tau^2 \Rightarrow \frac{1}{u_\tau}\frac{dU}{dy} = \frac{\rho u_\tau}{\mu}$$

Integration from wall to y:

$$\frac{U}{u_\tau} = \frac{\rho u_\tau y}{\mu} + C \qquad U(0) = 0 \Rightarrow U^+ = y^+$$

Log-layer

$$\boxed{U^+ = \frac{1}{\kappa}\ln(y^+) + B}$$

Log-law or Law of the wall

”Derivation” of log-law using Prandtl model

Prandtl model: $\mu_t = \rho l_{mix}^{\;2} \dfrac{dU}{dy}$

In log-layer: $\boxed{-\rho\langle u'v'\rangle \approx \tau_w}$ ➡ $\tau_w \approx \mu_t \dfrac{\partial U}{\partial y}$

$$\left.\begin{aligned} \tau_w &= \rho l_{mix}^{\;2}\left(\frac{dU}{dy}\right)^2 \\ \tau_w &= \rho u_\tau^2 \end{aligned}\right\} \Rightarrow u_\tau^2 = l_{mix}^{\;2}\left(\frac{dU}{dy}\right)^2 \qquad \boxed{u_\tau = l_{mix}\frac{dU}{dy}}$$

$$\boxed{l_{mix} = \kappa y}$$

$$\frac{u_\tau}{\kappa y} = \frac{dU}{dy} \Rightarrow \frac{1}{\kappa y^+} = \frac{dU^+}{dy^+} \qquad \boxed{U^+ = \frac{1}{\kappa}\ln(y^+) + B}$$

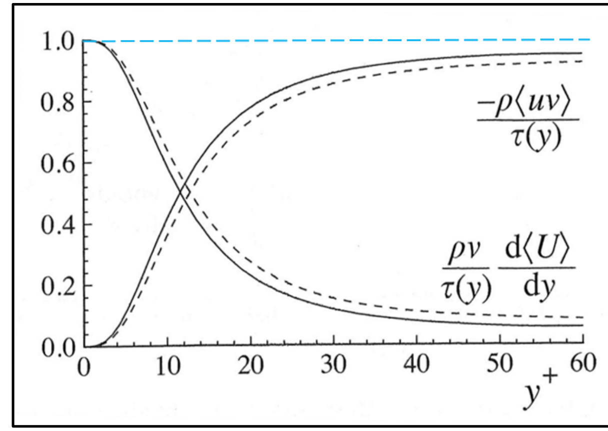

Relevant stresses in a 2D-boundary layer:

Boussinesq hypothesis

$$R_{12} = \mu_t \frac{\partial U}{\partial y}$$

Reynolds stress

$$R_{12} \equiv -\rho\langle u'v'\rangle$$

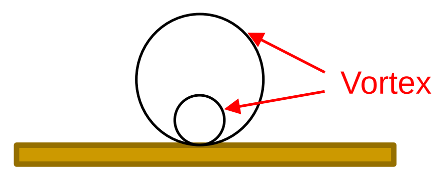

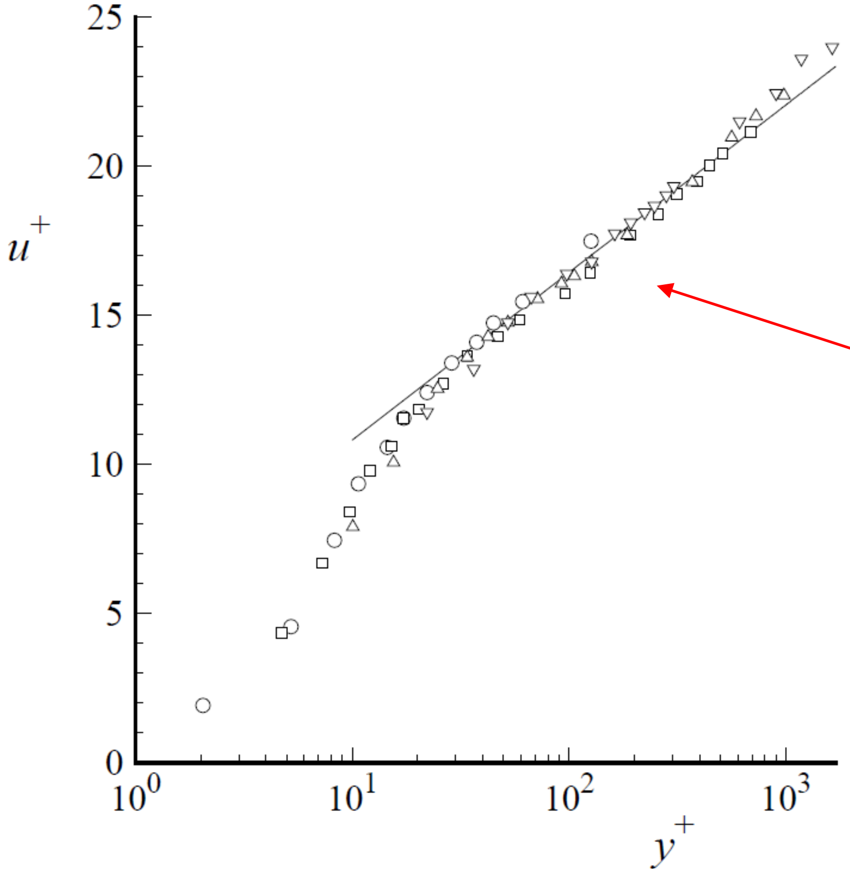

Figure 7.7: Mean velocity profiles in fully-developed turbulent channel flow measured by Wei and Willmarth (1989): ○, $Re_0 = 2,970$; □, $Re_0 = 14,914$; △, $Re_0 = 22,776$; ▽, $Re_0 = 39,582$; line, the log law, Eqs. (7.43)–(7.44).

Log-law or
Law of the wall

$$\boxed{u^+ = \frac{1}{\kappa}\ln(y^+) + B}$$

The data collapse on the same curve

Universal behavior

From Pope Ch.7

Laminar channel flow data

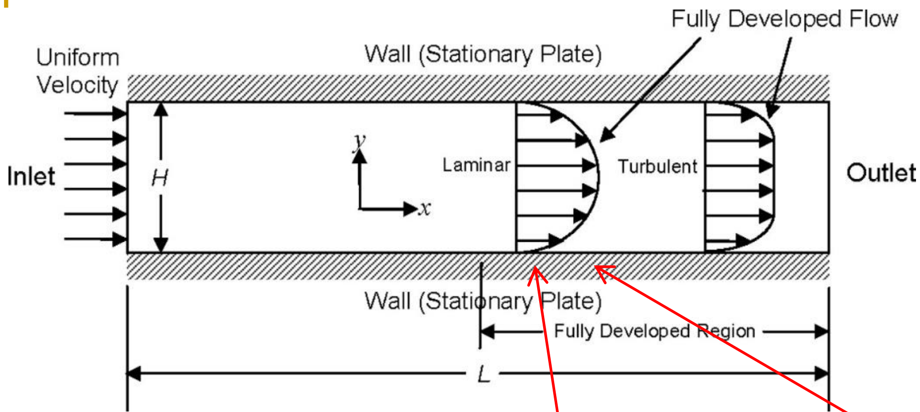

$H = 0.1\,m$

$L = 10\,m$

$$\left.\begin{aligned} \rho_{air} &= 1.2\ kg/m^3 \\ \mu_{air} &= 2\cdot 10^{-5}\ Pas \\ U_{in} &= 0.02\,m/s \end{aligned}\right\} \Rightarrow \mathrm{Re} = 120$$

$$\left.\begin{aligned} \rho_{water} &= 1000\ kg/m^3 \\ \mu_{water} &= 1\cdot 10^{-3}\ Pas \\ U_{in} &= 0.0012\,m/s \end{aligned}\right\} \Rightarrow \mathrm{Re} = 120$$

Channel flow: $U_{\max} = \frac{3}{2} U_{mean}$

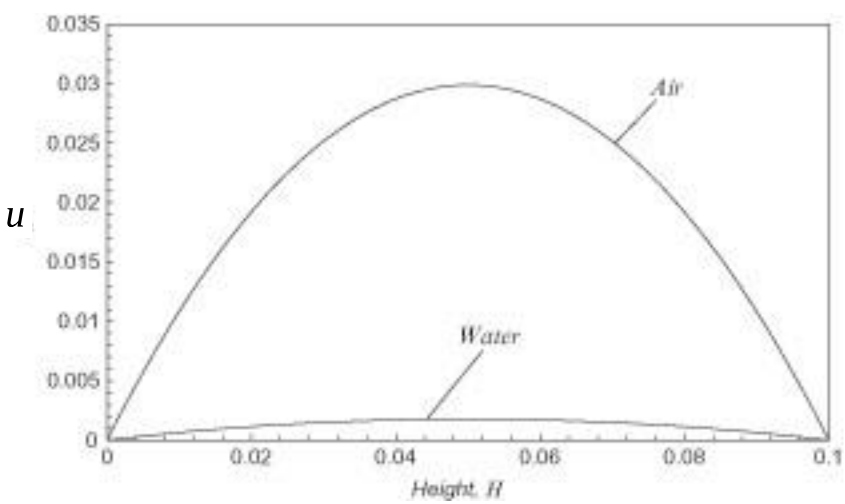

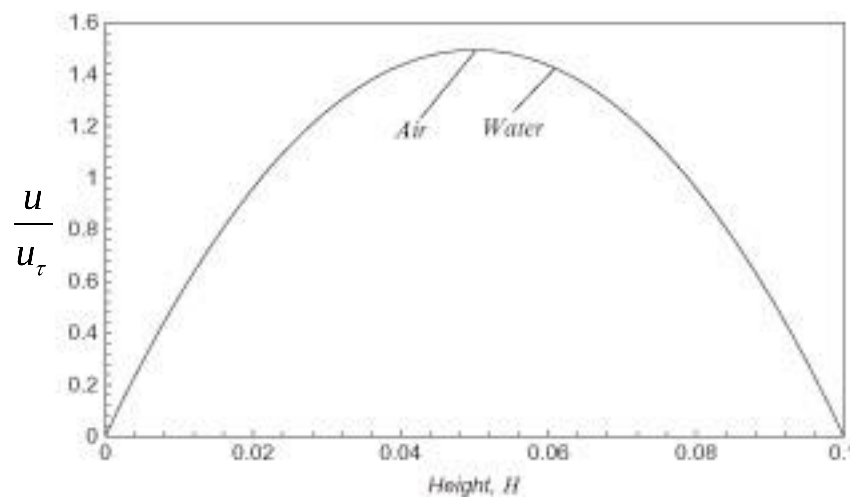

Turbulent channel flow data

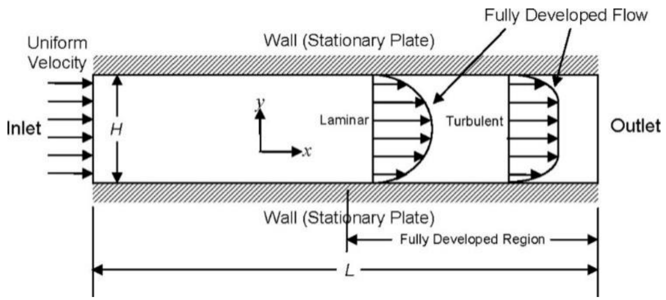

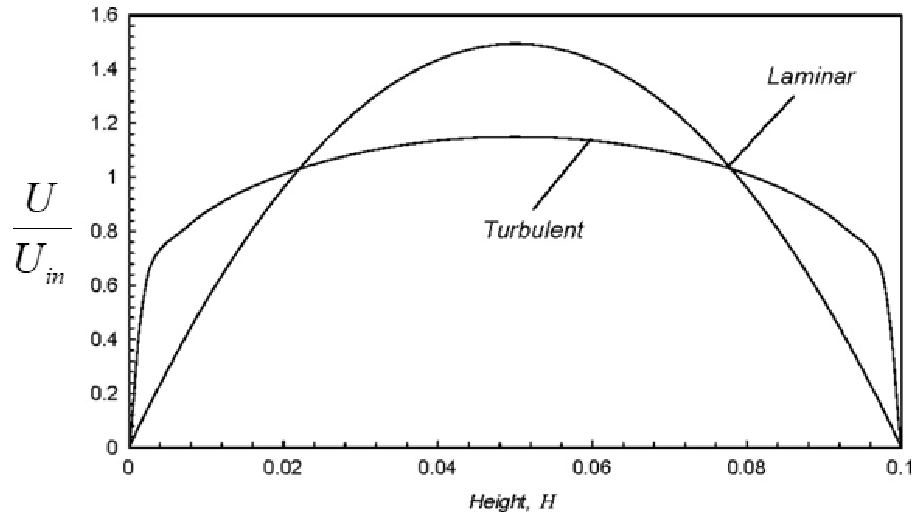

- The high turbulent viscosity in the center implies effective diffusion and is the reason why the turbulent velocity profile is so blunt

- Note that very near the walls the turbulent stress is smaller then the molecular viscous stress

- Note the huge difference between turbulent and laminar viscosity

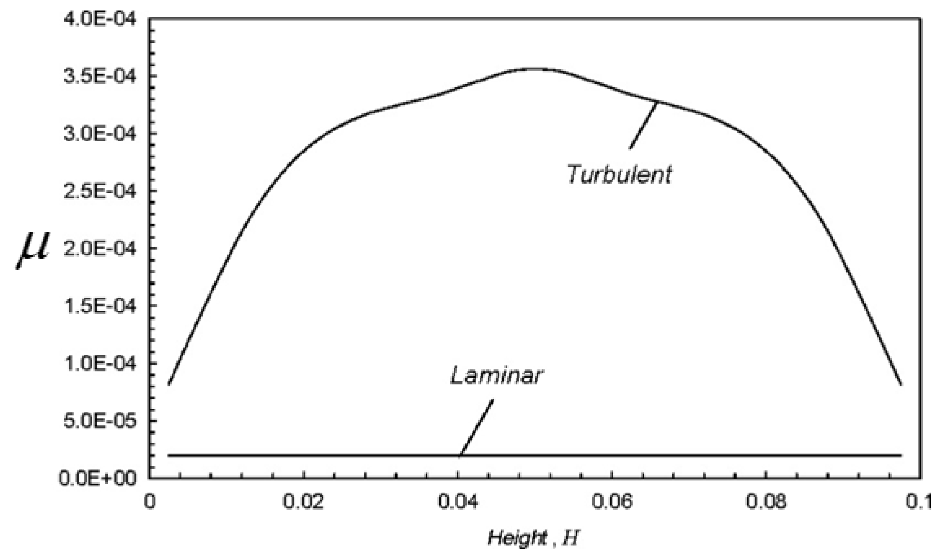

Turbulent channel flow data (cont.)

- The turbulent kinetic energy is zero at the wall as expected
- Note that also the dissipation is zero at the wall…

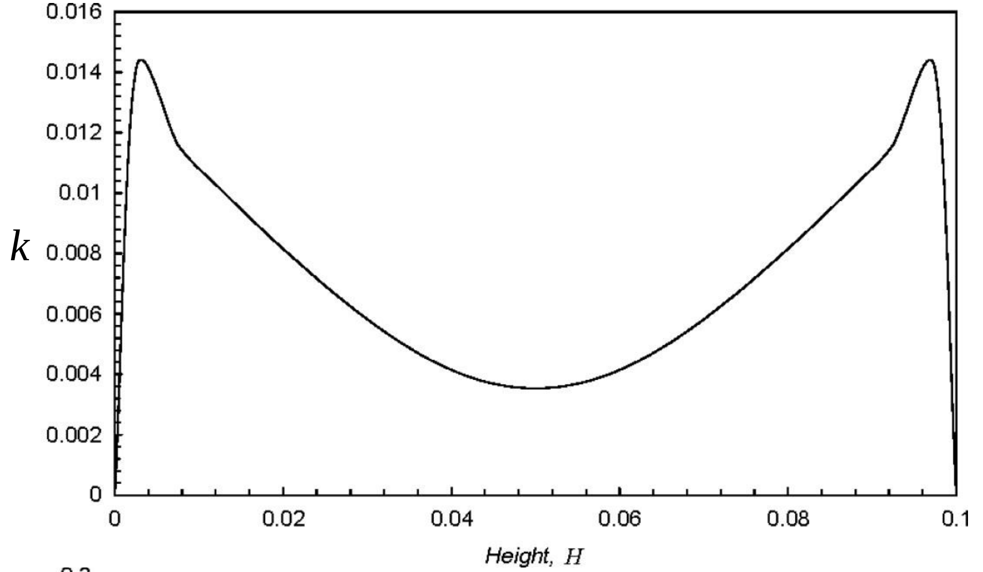

A common numerical approach:

$$\boxed{\tilde{\varepsilon} = \varepsilon - \varepsilon_0}$$

$\tilde{\varepsilon}$

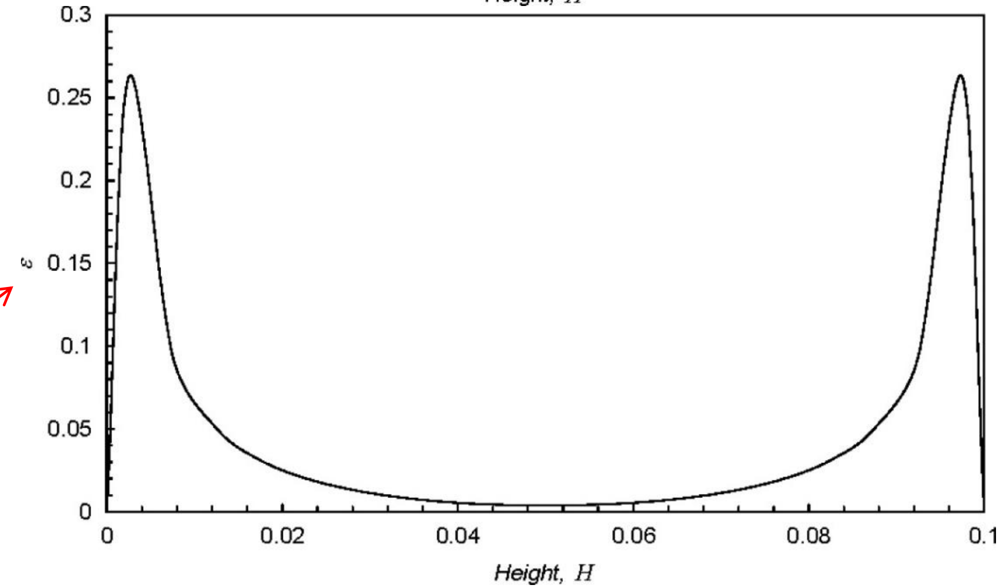

The standard *k-ε* model v.s. Experiment

Model k-equation

$$\frac{Dk}{Dt} = P_k - \varepsilon + D_k$$

Model ε-equation

$$\frac{D\varepsilon}{Dt} = \frac{\varepsilon}{k}\left(C_{\varepsilon 1} P_k - C_{\varepsilon 2}\varepsilon\right) + D_\varepsilon$$

Turbulent viscosity model

$$\boxed{\mu_t = C_\mu \rho \frac{k^2}{\varepsilon}}$$

From where?

$$C_\mu = 0.09$$

$$C_{\varepsilon 1} = 1.44 \quad C_{\varepsilon 2} = 1.92$$

$$\sigma_k = 1.0 \quad \sigma_\varepsilon = 1.3$$

Closure constants (Launder and Sharma)

k-production

$$P_k \equiv \frac{R_{ij}}{\rho}\frac{\partial U_i}{\partial x_j} = \frac{\mu_t}{\rho} S^2$$

k-diffusion

$$D_k \equiv \frac{\partial}{\partial x_j}\left[\frac{1}{\rho}\left(\mu + \frac{\mu_t}{\sigma_k}\right)\frac{\partial k}{\partial x_j}\right]$$

Dissipation

$$\varepsilon \equiv \frac{\mu}{\rho}\left\langle \frac{\partial u_i'}{\partial x_j}\frac{\partial u_i'}{\partial x_j}\right\rangle$$

ε-diffusion

$$D_\varepsilon \equiv \frac{\partial}{\partial x_j}\left[\frac{1}{\rho}\left(\mu + \frac{\mu_t}{\sigma_\varepsilon}\right)\frac{\partial \varepsilon}{\partial x_j}\right]$$

Wind tunnel designs

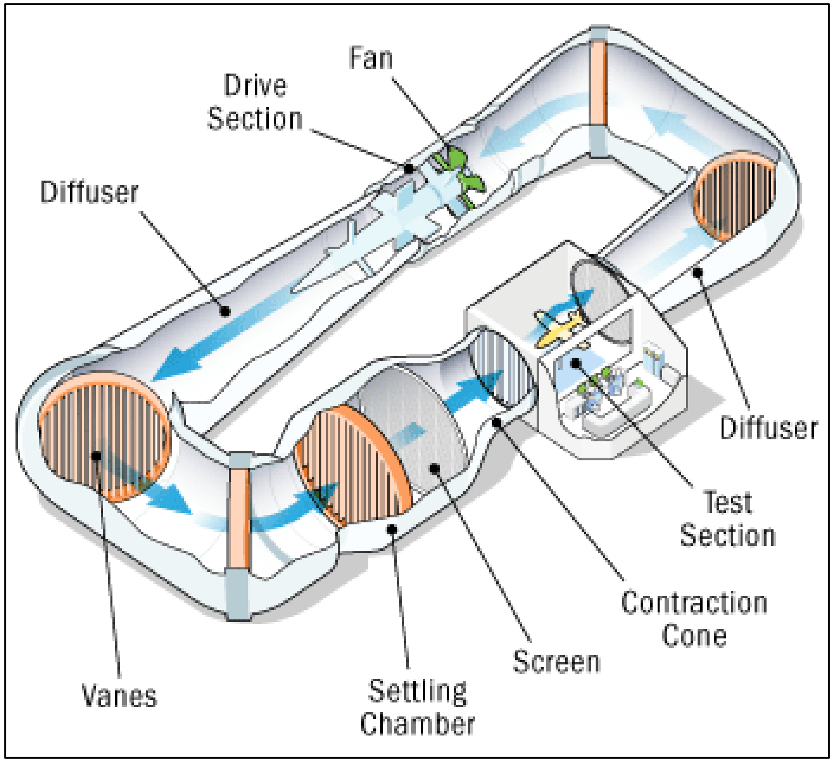

Flow straighteners (e.g. vanes)

- Reduces very effectively cross-stream components of the flow
- Usually a length about 10 cell diameters

Screens (mesh)

- Effective in breaking up larger eddies
- Reduces mean flow non-uniformities and streamwise fluctuations
- Some reduction in cross-stream components

Contraction

- Effective in reducing streamwise fluctuations and in particularly mean velocity variations
- Placed before the test section

Directly after the screens more small scale turbulence has been generated. This turbulence decays along the flow and such situation can be modeled.

Wind tunnel designs (cont)

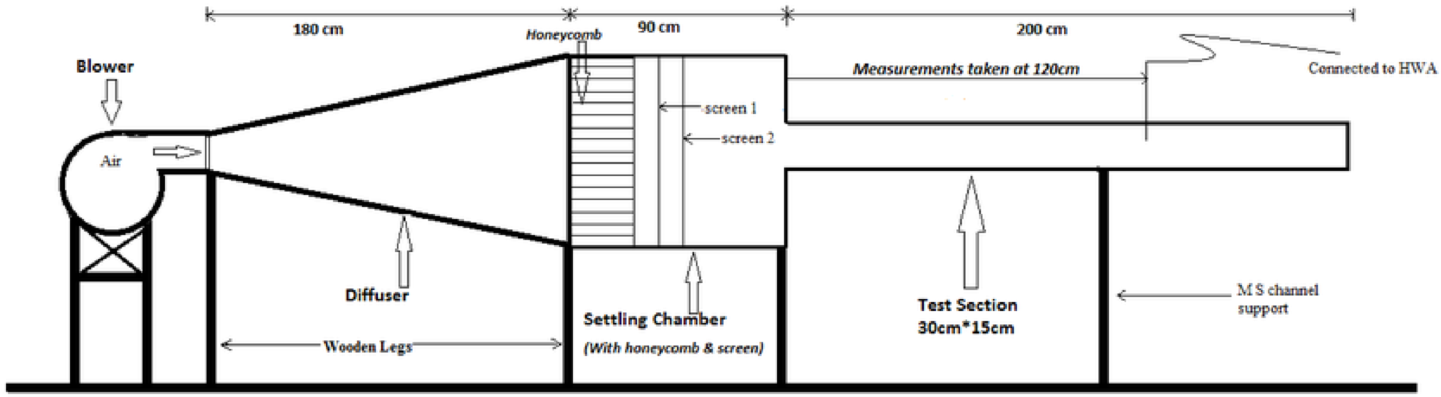

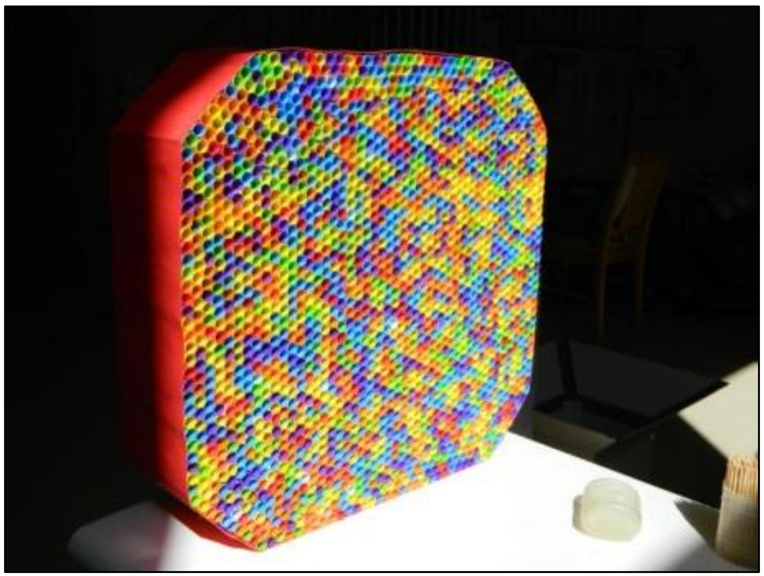

Flow straightener using straws

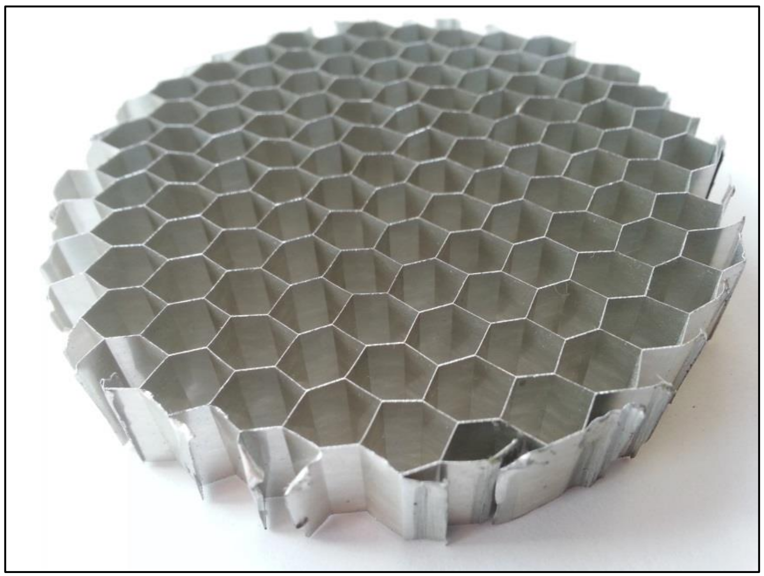

Flow straightener using honeycombs

The standard *k-ε* model : Homogeneous turbulence

Homogeneous turbulence: $$\boxed{\frac{\partial k}{\partial x_j} = \frac{\partial \varepsilon}{\partial x_j} = 0}$$

Model k-equation

$$\frac{Dk}{Dt} = P_k - \varepsilon + D_k$$

Model ε-equation

$$\frac{D\varepsilon}{Dt} = \frac{\varepsilon}{k}\left(C_{\varepsilon 1} P_k - C_{\varepsilon 2}\varepsilon\right) + D_\varepsilon$$

$$\frac{\partial k}{\partial t} = P_k - \varepsilon$$

$$\frac{\partial \varepsilon}{\partial t} = \frac{\varepsilon}{k}\left(C_{\varepsilon 1} P_k - C_{\varepsilon 2}\varepsilon\right)$$

$C_\mu = 0.09$

$C_{\varepsilon 1} = 1.44 \quad C_{\varepsilon 2} = 1.92$

$\sigma_k = 1.0 \quad \sigma_\varepsilon = 1.3$

Closure constants (Launder and Sharma)

We will now investigate how to determine:

1) $C_{\varepsilon 2}$

2) $C_{\varepsilon 1}$

Case 1. Decaying turbulence

No mean velocity gradients

$\Rightarrow \quad P_k = 0$

Obtained in wind tunnel experiments after flow through a screen or grid

$$P_k \equiv R_{ij} \frac{\partial U_i}{\partial x_j}$$

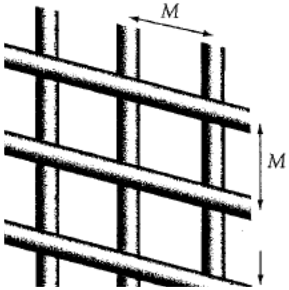

Experimental data

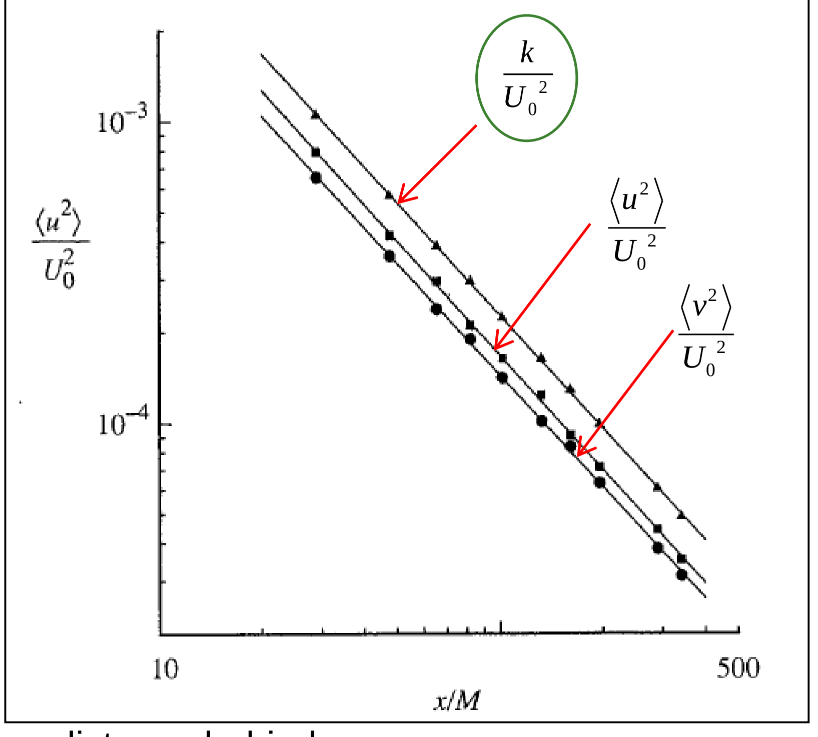

x=distance behind screen

Empirical model

$$\Rightarrow \quad \boxed{\frac{k}{U_0^2} = A\left(\frac{x}{M}\right)^{-n}} \qquad n \approx 1.3$$

Consider now a moving frame of reference $(x = tU_0)$

$$\Rightarrow \quad \frac{k}{U_0^2} = A\left(\frac{U_0}{M}\right)^{-n} t^{-n}$$

$$\Rightarrow \quad k = k_0\left(\frac{t}{t_0}\right)^{-n} \qquad k_0 \equiv AU_0^2\left(\frac{U_0}{M}\right)^{-n} t_0^{-n}$$

As expected, no production means that the turbulence decreases in time.

Case 1. Decaying turbulence (cont.)

Grid turbulence: $P_k = 0$ $\Rightarrow$ $\boxed{\dfrac{\partial k}{\partial t} = -\varepsilon \,, \quad \dfrac{\partial \varepsilon}{\partial t} = -C_{\varepsilon 2}\dfrac{\varepsilon^2}{k}}$

$$\left.\begin{aligned} k(t) &= k_0\left(\frac{t}{t_0}\right)^{-n} \\ \frac{\partial k}{\partial t} &= -\varepsilon \end{aligned}\right\} \Rightarrow \quad \varepsilon(t) = \varepsilon_0\left(\frac{t}{t_0}\right)^{-(n+1)}$$

(Exercise)

$$t_0 = n\frac{k_0}{\varepsilon_0}$$

$$\frac{\partial \varepsilon}{\partial t} = -C_{\varepsilon 2}\frac{\varepsilon^2}{k} \quad \Rightarrow \quad n = \frac{1}{C_{\varepsilon 2} - 1}$$

(Exercise)

$$C_{\varepsilon 2} = \frac{n+1}{n}$$

$\boxed{n \approx 1.3 \quad \Rightarrow \quad C_{\varepsilon 2} \approx 1.78}$

Closure constants
(Launder and Sharma)

$$\boxed{\begin{array}{ll} C_\mu = 0.09 & \\ C_{\varepsilon 1} = 1.44 & C_{\varepsilon 2} = 1.92 \\ \sigma_k = 1.0 & \sigma_\varepsilon = 1.3 \end{array}}$$

Case 2. Homogeneous shear flow

Can be achieved in wind tunnel experiment with a **non-uniform** screen followed by a flow straightener section

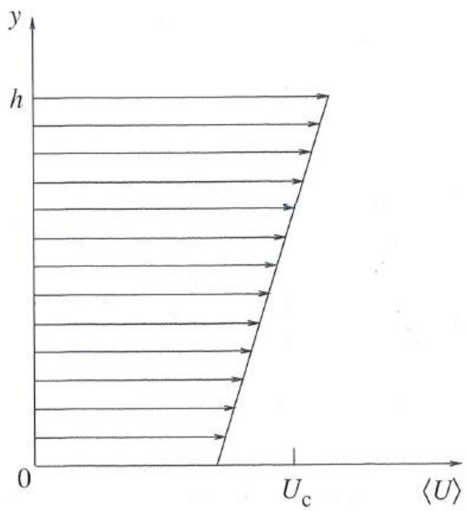

Assume

$$S = \frac{dU}{dy} = const.$$

Table 5.4. *Statistics in homogeneous turbulent shear flow from the experiments of Tavoularis and Corrsin (1981) and the DNS of Rogers and Moin (1987)*

	Tavoularis and Corrsin		Rogers and Moin
	$x/h = 7.5$	$x/h = 11.0$	$\mathcal{S}t = 8.0$
$\langle u^2 \rangle / k$	1.04	1.07	1.06
$\langle v^2 \rangle / k$	0.37	0.37	0.32
$\langle w^2 \rangle / k$	0.58	0.56	0.62
$-\langle uv \rangle / k$	0.28	0.28	0.33
$-\rho_{uv}$	0.45	0.45	0.57
$\mathcal{S}k/\varepsilon$	6.5	6.1	4.3
$\mathcal{P}/\varepsilon$	1.8	1.7	1.4
$L_{11}\mathcal{S}/k^{1/2}$	4.0	4.0	3.7
$L_{11}/(k^{3/2}/\varepsilon)$	0.62	0.66	0.86

These two columns corresponds to measuring at two points downstream

Case 2: Homogeneous shear flow (cont.)

Experimental results:
(see Table 5.4)

$$\frac{dU}{dy}\frac{k}{\varepsilon} \approx 6.1, \quad \frac{P_k}{\varepsilon} \approx 1.7$$

$$\frac{dU}{dy}\frac{k}{\varepsilon} = const \;\Rightarrow\; \frac{k}{\varepsilon} = const$$

$$\frac{\partial k}{\partial t} = P_k - \varepsilon \qquad \frac{\partial \varepsilon}{\partial t} = C_{\varepsilon 1}\frac{\varepsilon}{k}P_k - C_{\varepsilon 2}\frac{\varepsilon^2}{k}$$

$$\Downarrow$$

$$\frac{\partial}{\partial t}\left(\frac{k}{\varepsilon}\right) = \left(C_{\varepsilon 2} - 1\right) - \left(C_{\varepsilon 1} - 1\right)\left(\frac{P_k}{\varepsilon}\right)$$

$\frac{k}{\varepsilon}$ constant in time $\Rightarrow$ $\left(C_{\varepsilon 1} - 1\right) = \dfrac{\left(C_{\varepsilon 2} - 1\right)}{\left(\dfrac{P_k}{\varepsilon}\right)}$

$$\frac{P_k}{\varepsilon} \approx 1.7, \quad C_{\varepsilon 2} = 1.92 \quad \Rightarrow \quad C_{\varepsilon 1} = 1.54$$

Closure constants
(Launder and Sharma)

$$C_\mu = 0.09$$
$$C_{\varepsilon 1} = 1.44 \qquad C_{\varepsilon 2} = 1.92$$
$$\sigma_k = 1.0 \qquad \sigma_\varepsilon = 1.3$$

CFD benchmark test: The round Jet

“Direct Numerical Simulation of Subsonic Round Turbulent Jet”
Z. Wang etal. 2010

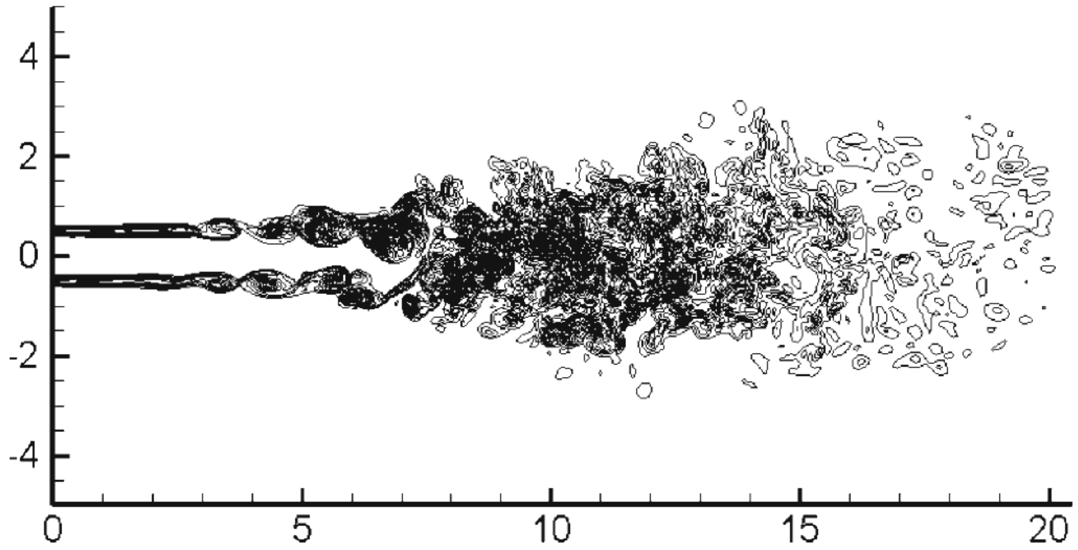

Fig. 2 Instantaneous contour plot of vorticity magnitude at plane z=0

Fig. 3 Instantaneous image of quantity Q of jet. Q=17

Fluctuation Energy budget in a round jet (cont)

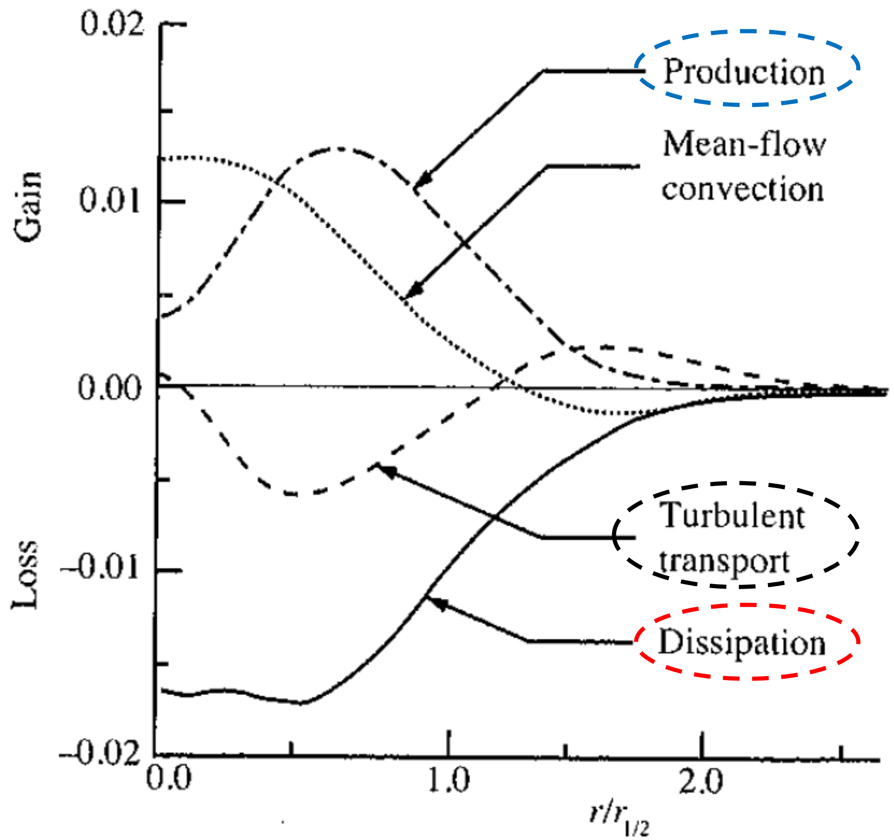

Fig. 5.16. The turbulent-kinetic-energy budget in the self-similar round jet. Quantities are normalized by U_0 and $r_{1/2}$. (From Panchapakesan and Lumley (1993a).)

Study group exercise

From Pope, 2000

Free turbulence data: The Round Jet

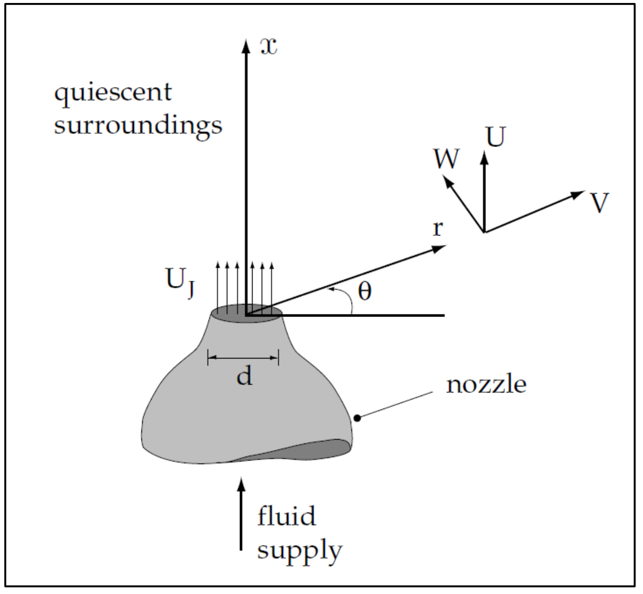

Spreading rate

$$\boxed{SR \equiv \frac{dr_{1/2}}{dx}}$$

From Pope, "Turbulent flows"

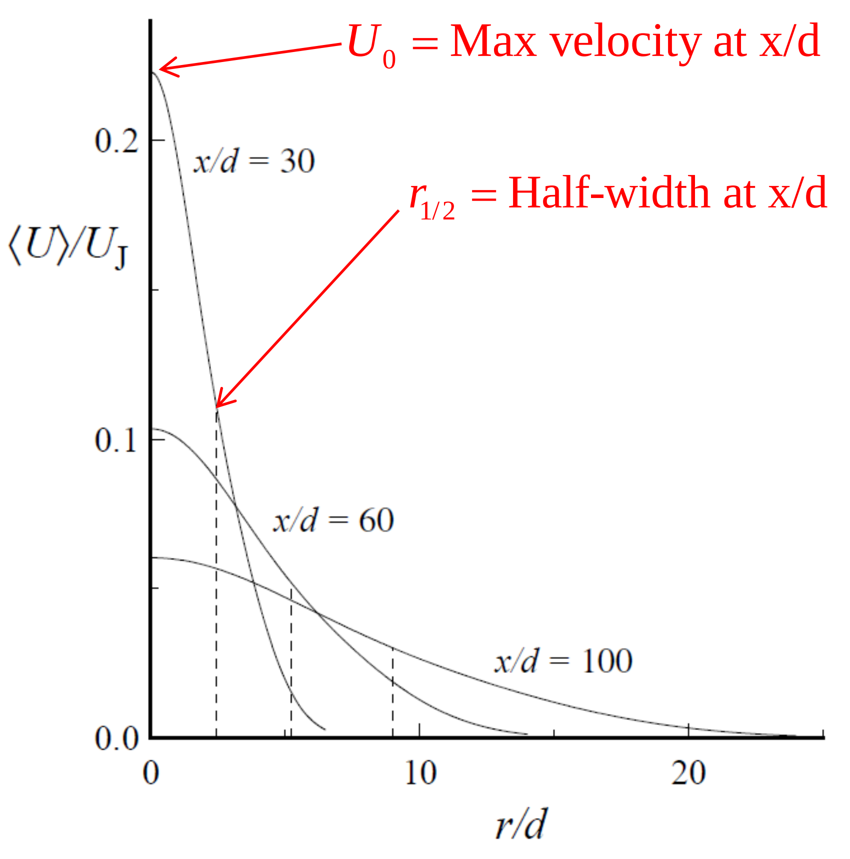

Figure 5.2: Radial profiles of mean axial velocity in a turbulent round jet, Re = 95, 500. The dashed lines indicate the half-width, $r_{\frac{1}{2}}(x)$, of the profiles. (Adapted from the data of Hussein et al. (1994).)

Dimensionless plot: Self-similarity of a round jet

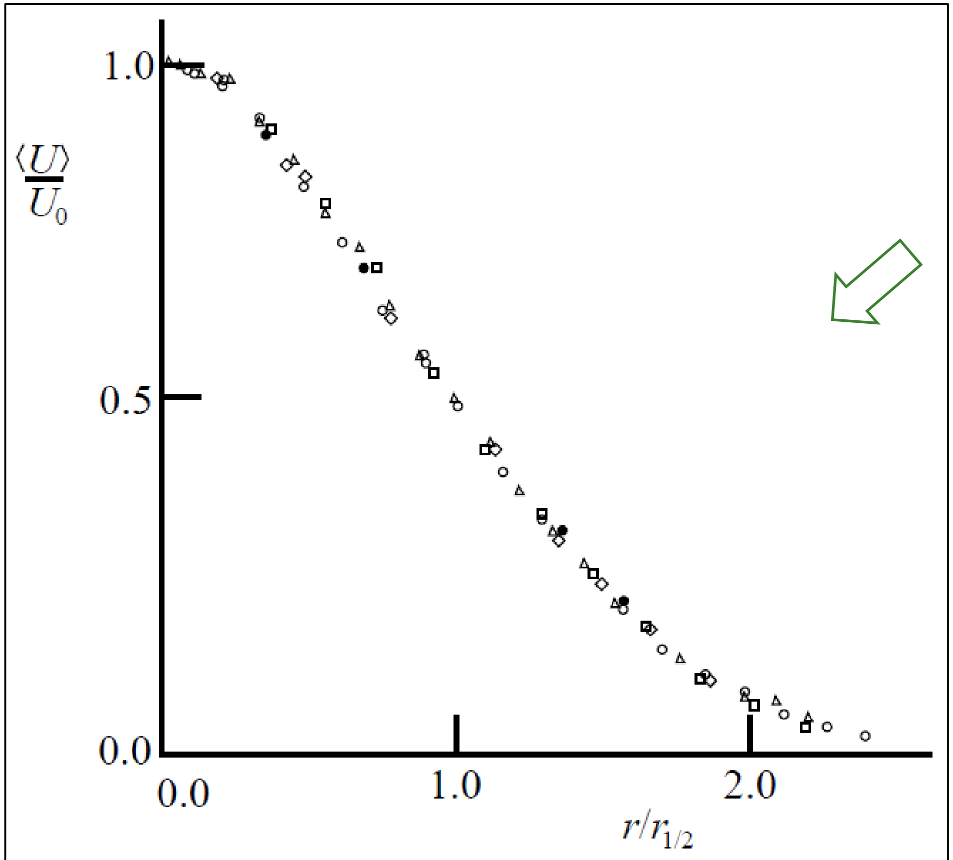

Figure 5.3: Mean axial velocity against radial distance in a turbulent round jet, Re $\approx 10^5$; measurements of Wygnanski and Fiedler (1969). Symbols: $\circ$, $x/d = 40$; $\triangle$, 50; $\square$, 60; $\diamond$, 75; $\bullet$, 97.5.

- Scale velocity by U_0
- Scale radial distance by $r_{1/2}$

The data is overlapping when scaled in this way

Indicating a universal form of the graph

In this scaling the velocity profile is self-similar

CFD benchmark test: Spreading rate in a Round Jet

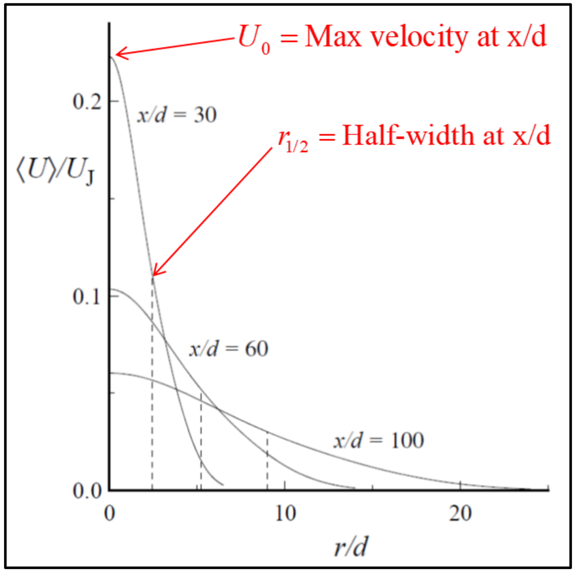

Spreading rate

$$SR \equiv \frac{dr_{1/2}}{dx}$$

From ”Modeling of turbulent free shear flows”, NASA

Activation of vortex streching mechanism

Table 2: Free shear flow spread rates predicted by RANS models.

		Mixing Layer	Plane Jet	Round Jet	Radial Jet	Wake
	Experiment[7, 78–81]	0.103-0.120	0.100-0.110	0.086-0.096	0.096-0.110	0.320-0.400
$k-\omega$	Wilcox[82*]	0.096	0.108	0.094	0.099	0.326
$k-\omega$	Wilcox[83*]	0.105	0.101	0.088	0.099	0.339
$k-\omega$	Wilcox[84*]	0.141	0.135	0.369	0.317	0.496
SST	Menter[85†]	0.100	0.112	0.127	-	0.257
$k-\epsilon$	Launder & Sharma[77*]	0.098	0.109	0.120	0.094	0.256
	with Pope[86*]	0.098	0.109	0.086	0.040	0.256
$k-\zeta$	Robinson, et al.[87*]	0.112	0.115	0.091	0.097	0.313
$k-\tau$	Speziale, et al.[88*]	0.082	0.089	0.102	0.073	0.221
SA	Spalart & Allmaras[76*]	0.109	0.157	0.248	0.166	0.341

Centerline mean velocity variations of a round jet

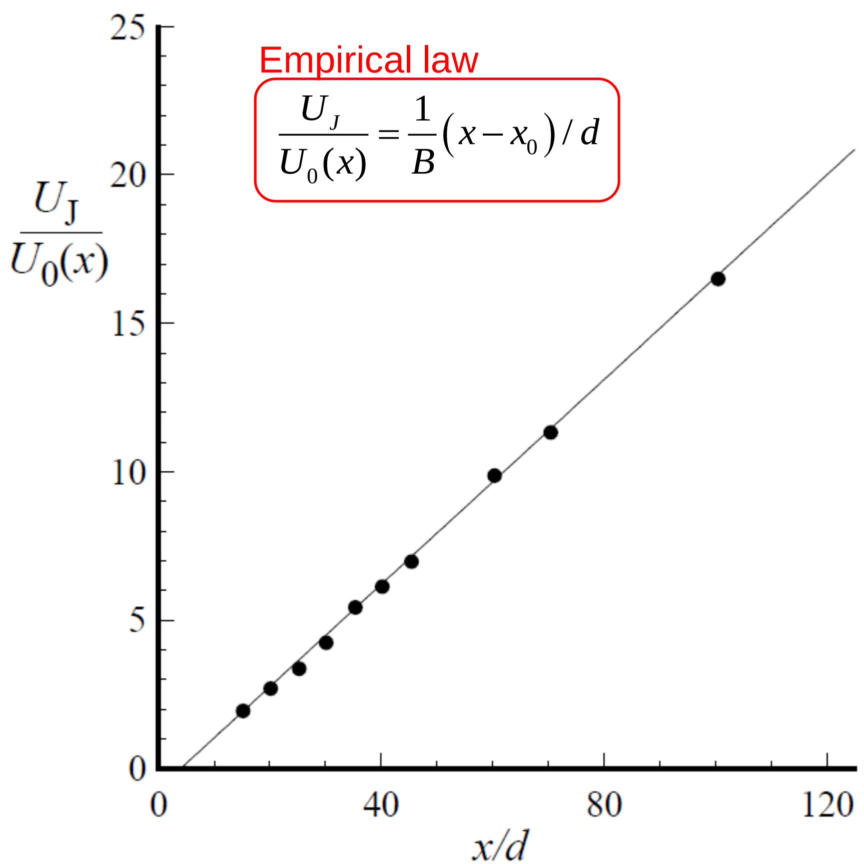

Figure 5.4: Centerline mean velocity variation with axial distance in a turbulent round jet, Re = 95, 500: symbols, experimental data of Hussein et al. (1994), line—Eq. (5.6) with $x_0/d = 4$, $B = 5.8$.

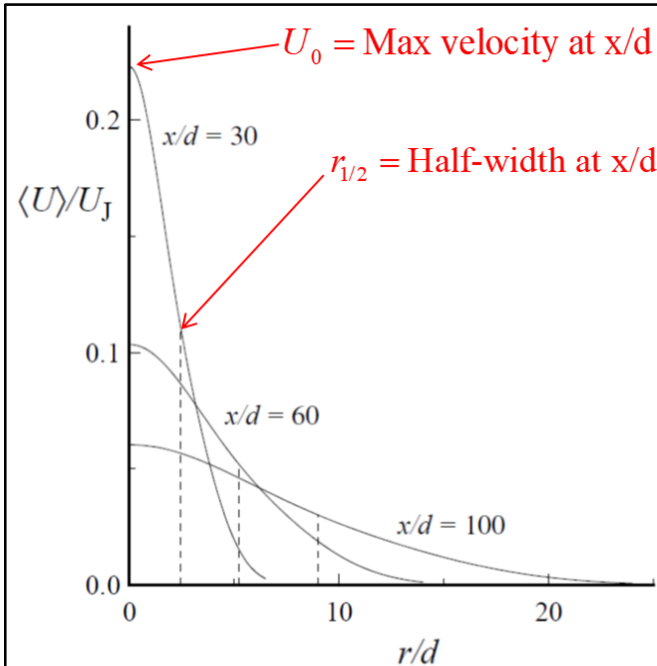

Lateral velocity of a round jet

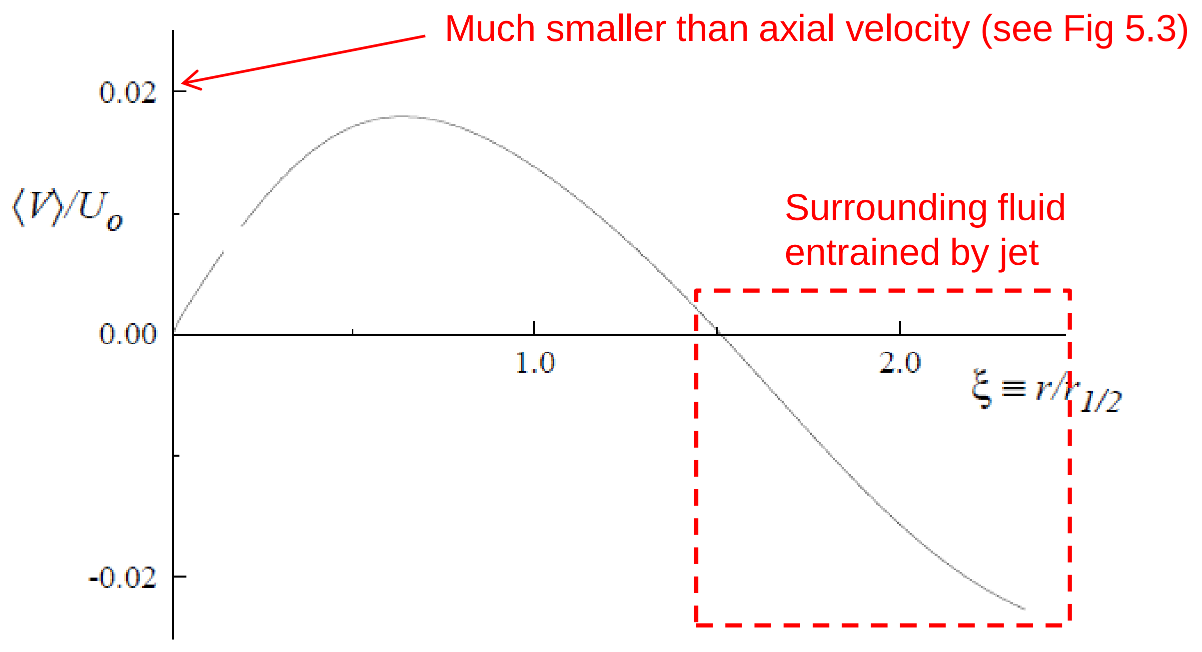

Figure 5.6: Mean lateral velocity in the self-similar round jet. From the LDA data of Hussein et al. (1994).

Reynolds stresses

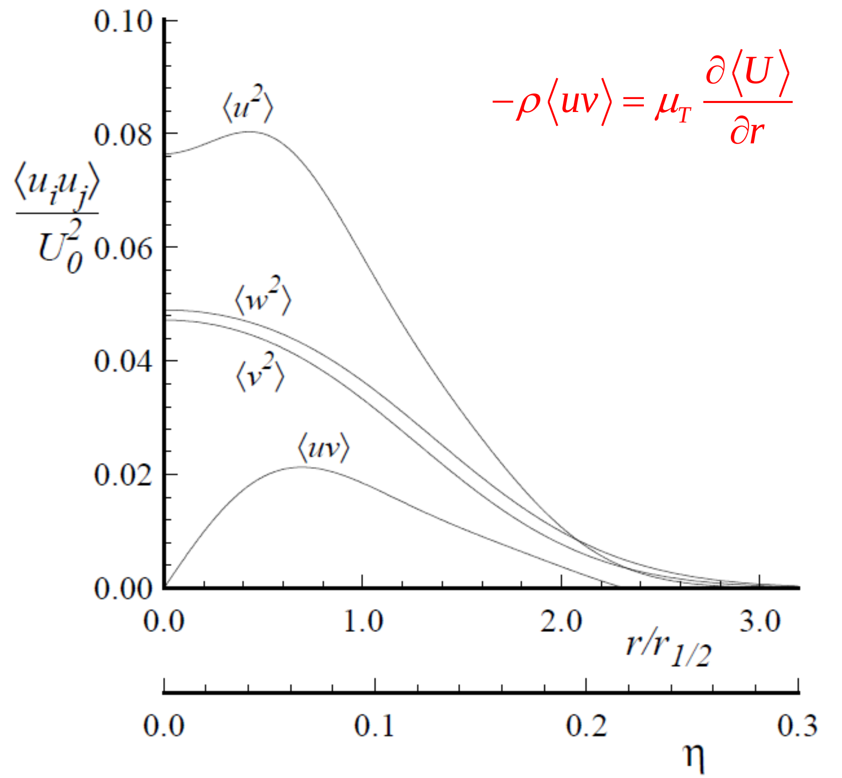

Figure 5.7: Profiles of Reynolds stresses in the self-similar round jet. Curve fit to the LDA data of Hussein et al. (1994).

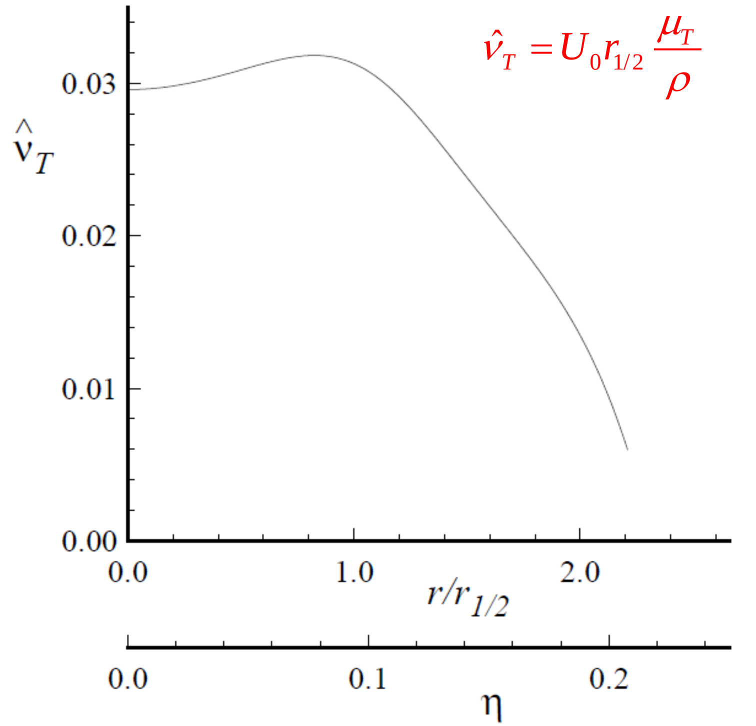

Figure 5.10: Normalized turbulent diffusivity $\hat{\nu}_T$ (Eq. (5.34)) in the self-similar round jet. From the curve fit to the experimental data of Hussein et al. (1994).

Spreading Rate dependency on Re?

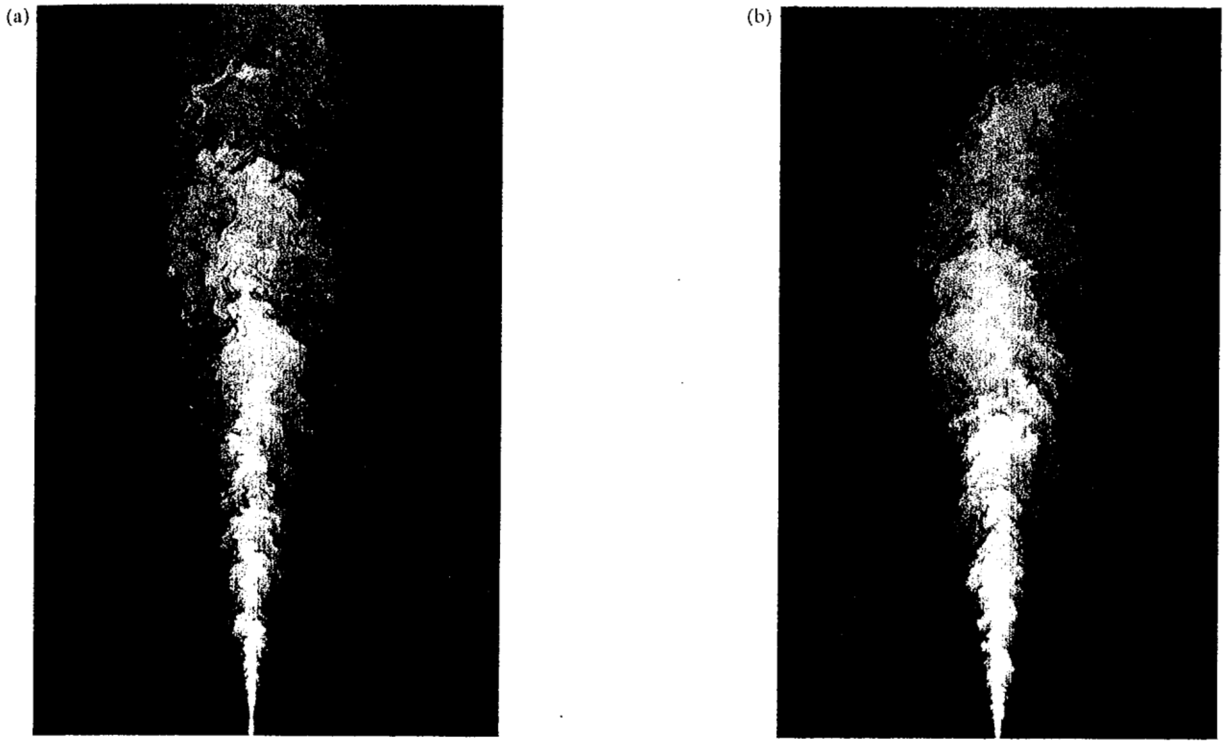

Fig. 1.2. Planar images of concentration in a turbulent jet: (a) Re = 5,000 and (b) Re = 20,000. From Dahm and Dimotakis (1990).

	Panchapakesan and Lumley (1993a)	Hussein *et al.* (1994), hot-wire data	Hussein *et al.* (1994), laser-Doppler data
Re	11,000	95,500	95,500
S	0.096	0.102	0.094
B	6.06	5.9	5.8

End of lecture